ResearchGate

See discussions, stats, and author profiles for this publication at: https://www.researchgate.net/publication/285420255

Numerical modeling of dam-break flow impacting on flexible structures using an improved SPH-EBG method

Article *in* Coastal Engineering · February 2016

DOI: 10.1016/j.coastaleng.2015.11.007

CITATIONS
3

READS
195

4 authors, including:

Xiufeng Yang
Iowa State University
16 PUBLICATIONS **77** CITATIONS
SEE PROFILE

Shiliu Peng
institute of mechanics, CAS
4 PUBLICATIONS **18** CITATIONS
SEE PROFILE

Chenguang Huang
Chinese Academy of Sciences
117 PUBLICATIONS **365** CITATIONS
SEE PROFILE

Some of the authors of this publication are also working on these related projects:

Laser shock phenomena View project

All content following this page was uploaded by Xiufeng Yang on 02 February 2016.

The user has requested enhancement of the downloaded file. All in-text references underlined in blue are added to the original document and are linked to publications on ResearchGate, letting you access and read them immediately.

Coastal Engineering 108 (2016) 56–64

Contents lists available at ScienceDirect

Coastal Engineering

journal homepage: www.elsevier.com/locate/coastaleng

Numerical modeling of dam-break flow impacting on flexible structures using an improved SPH–EBG method

Xiufeng Yang [a,b,*], Moubin Liu [c], Shiliu Peng [a], Chenguang Huang [a]

[a] Institute of Mechanics, Chinese Academy of Sciences, Beijing 100190, China
[b] Department of Mechanical Engineering, Iowa State University, Ames, IA 50011, USA
[c] College of Engineering, Peking University, Beijing 100871, China

ARTICLE INFO

Article history:
Received 18 August 2015
Accepted 11 November 2015
Available online 1 December 2015

Keywords:
Fluid–structure interaction
Flexible structure
Numerical modeling
Smoothed particle hydrodynamics
Element boundary group

ABSTRACT

An improved coupling method of smoothed particle hydrodynamics (SPH) and element bending group (EBG) is developed for modeling the interaction of viscous flows with free surface and flexible structures with free and fixed ends. SPH and EBG are both particle methods which are appealing in modeling problems with free surfaces, moving interfaces and large deformations. SPH is used to model viscous fluid, while EBG is used to model flexible structure. Structure particles are also used as moving boundary for SPH, and the interaction of flexible structure with fluid is therefore modeled through the interaction of structure particles and fluid particles. A fixed-end treatment is introduced for flexible structures. A free surface treatment and a surface tension model are used for free surface flow. The improved SPH–EBG method is applied to simulate problems of dam break flow on flexible structures. The good agreement of presented numerical results with existing experimental and numerical results clearly demonstrates the effectiveness of the SPH and EBG coupling approach in modeling fluid–flexible structure interactions.

© 2015 Elsevier B.V. All rights reserved.

1. Introduction

There are many examples of fluid–structure interactions in nature, coastal and ocean engineering. How to accurately model the interaction of fluids and structures is of great importance both in engineering and scientific research. Numerical methods to model fluid–structure interactions have been developed for decades. If the deformation of a structure is very small, the structure is usually treated as a rigid structure. If the deformation of a structure is large, it should be considered in numerical simulations. Although the modeling of fluid–structure interactions has been studied for several decades, it is still a challenging work to model the interactions of fluids and flexible structures. The numerical difficulty in modeling fluid–flexible structure interaction is the treatment of moving interfaces and deformable boundaries. Due to the complexity of the problem, there are only a limited number of literatures describing the numerical modeling of flexible structures interacting with fluid flows (Hosseini and Feng, 2009; Idelsohn et al., 2008; Walhorn et al., 2005; Yu, 2005; Zhu and Peskin, 2003), and most of those numerical methods are based on mesh or grid. Walhorn et al. (2005) presented a space–time finite element method for fluid–structure interactions with level set method for free surfaces. Idelsohn et al. (2008) solved fluid–structure interactions using the particle finite element method. In order to model Newtonian fluid interacting slender bodies, a coupling method of fictitious domain and mortar element was developed (Baaijens, 2001). This method is suitable for complicated mesh movement in arbitrary Lagrangian–Eulerian (ALE) method. Antoci et al. (2007) simulated both fluid and structure using smoothed particle hydrodynamics (SPH) method.

A numerical method which can well model the interaction of a fluid with free surface and a structure with large deformation would be appealing in modeling fluid–flexible structure interactions. In this paper, an improved coupling method of SPH and element bending group (EBG) is developed for modeling the interaction of viscous fluid with free surface and flexible structure with large deformation.

SPH method is a Lagrangian meshfree particle method. It was first invented to solve astrophysical problems (Gingold and Monaghan, 1977; Lucy, 1977), and later extended to solve many other problems, especially fluid simulations (Breinlinger et al., 2013; Hu and Adams, 2007; Marrone et al., 2013; Morris et al., 1997). In SPH, a fluid is represented by a set of particles which move according to the governing equations of the fluid. Then the motion of the fluid is represented by the motion of the particles, and free surface or interface of multiphase flow moves with particles representing their phase defined at the initial stage. The meshfree nature of SPH method removes the difficulties due to large deformations since SPH uses particles rather than mesh as a computational frame to approximate related governing equations. Therefore, SPH is well suited for modeling fluid flows with free surfaces and moving interfaces.

* Corresponding author at: Institute of Mechanics, Chinese Academy of Sciences, Beijing 100190, China.
E-mail addresses: yangxf@imech.ac.cn (X. Yang), mbliu@pku.edu.cn (M. Liu).

http://dx.doi.org/10.1016/j.coastaleng.2015.11.007
0378-3839/© 2015 Elsevier B.V. All rights reserved.

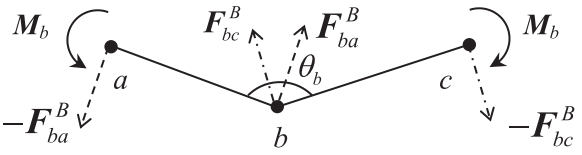

Fig. 1. An EBG is made of two adjacent line segments connecting three neighboring particles.

EBG technique can also be regarded as a particle method, and it was first proposed for modeling membrane structure which can be considered as an elastic shell (Zhou and Wagoner, 1995). Later it was extended to model red blood cell membrane (Hosseini and Feng, 2009; Tsubota et al., 2006). A flexible structure can also be modeled by EBG method. In EBG model, an EBG consists of two adjacent line segments connecting three neighboring particles. Except for the tension force, the bending moment needs to be considered when modeling the movement and deformation of a flexible structure. The bending moment on an EBG can be converted into pairs of forces acting on the neighboring particles. Hence the EBG method can be attractive in modeling the movement and deformation of flexible structures.

By coupling SPH with EBG, it is possible to model fluid–flexible structure interactions. The SPH method can be used to model viscous fluid flows, and the EBG method can be used to model the dynamic movement and deformation of flexible structures. Then the interaction of fluid and flexible structure can be modeled by the interaction of the neighboring fluid (SPH) and structure (EBG) particles. The idea of SPH–EBG coupling method was originally proposed by Hosseini and Feng (2009) to model red blood cell deformations in shear flows, and the reported numerical results demonstrate good consistence with the experimental observations. However, a red blood cell is a closed structure with no free end and no fixed end, and there is no free surface flow around it. Yang et al. (2014) extended SPH–EBG method to model a flexible fiber with two free ends immersed in a viscous flow. They studied the drag scaling law and bending modes of a flexible fiber centrally fixed in a viscous flow.

In the present work, the SPH–EBG method is extended to model the interaction of fluid with free surface and flexible structure with free and fixed ends. Some numerical techniques will be introduced for the SPH–EBG method, and these make the coupling method more powerful.

2. Numerical methodology

In SPH–EBG method, SPH is used to model fluid flow, and EBG is used to model flexible structure. In this section, the SPH and EBG methods will be introduced, respectively. Then the coupling of SPH and EBG will be described.

2.1. SPH method

The Navier–Stokes (N–S) equations are used for viscous fluid. The Lagrangian form of the N–S equations is written as follows

$$\frac{d\rho}{dt} = -\rho\nabla\cdot\mathbf{u} \tag{1}$$

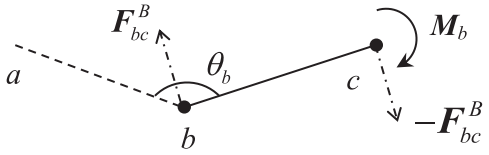

Fig. 2. Fixed end treatment. Assuming that there is a fixed line, *ab*, outside the fixed end *b*.

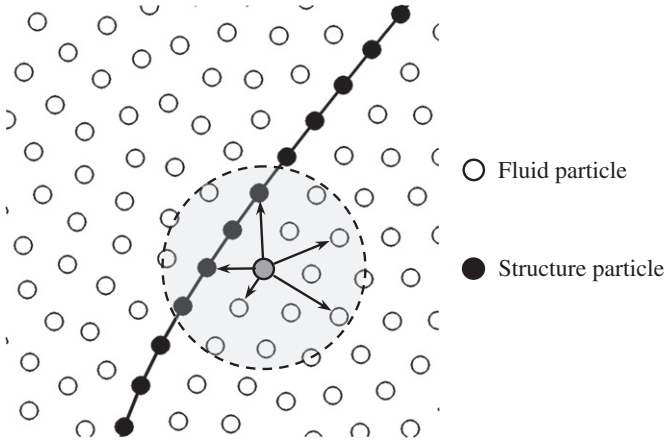

Fig. 3. Interaction of fluid and structure particles.

$$\frac{d\mathbf{u}}{dt} = \mathbf{g} - \frac{1}{\rho}\nabla p + \frac{\mu}{\rho}\nabla^2\mathbf{u} \tag{2}$$

where ρ is the fluid density, $\boldsymbol{u}$ is the fluid velocity, p is the fluid pressure, μ is the dynamic viscosity of the fluid, and $\boldsymbol{g}$ denotes the body force acting on the fluid.

In SPH method, a fluid is represented by a set of particles, which can move according to corresponding governing equations. Specifically, for any field variable, $A(\mathbf{r})$, which is a function of the spatial position $\boldsymbol{r}$, the value of function A at a certain point a whose position vector is $\boldsymbol{r}_a$ can be approximated by the following integral interpolation:

$$A(\mathbf{r}_a) = \int_\Omega A(\mathbf{r})W(\mathbf{r}_a - \mathbf{r}, h)dV \tag{3}$$

where $W(\mathbf{r}_a - \mathbf{r}, h)$ is a smoothing or kernel function, h is a smoothing length, dV is a differential volume element, and Ω is an integral domain. When representing a fluid domain with discrete SPH particles while the volume of each particle can be represented by m/ρ, the interpolation is approximated by a summation interpolation over particles:

$$A_a = \sum_b A_b W_{ab}\frac{m_b}{\rho_b} \tag{4}$$

where $W_{ab} = W(\mathbf{r}_a - \mathbf{r}_b, h)$, the indexes a and b denote labels of particles. The summation is taken over all particles, but in practice it is only

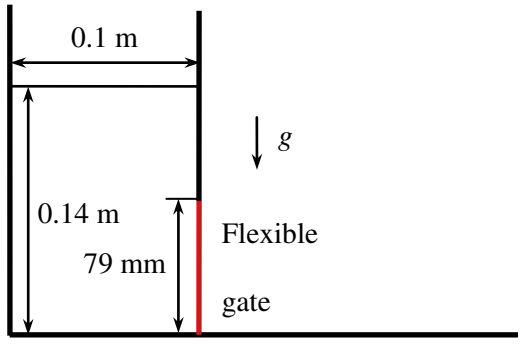

Fig. 4. Sketch of dam break with a top-fixed flexible gate.

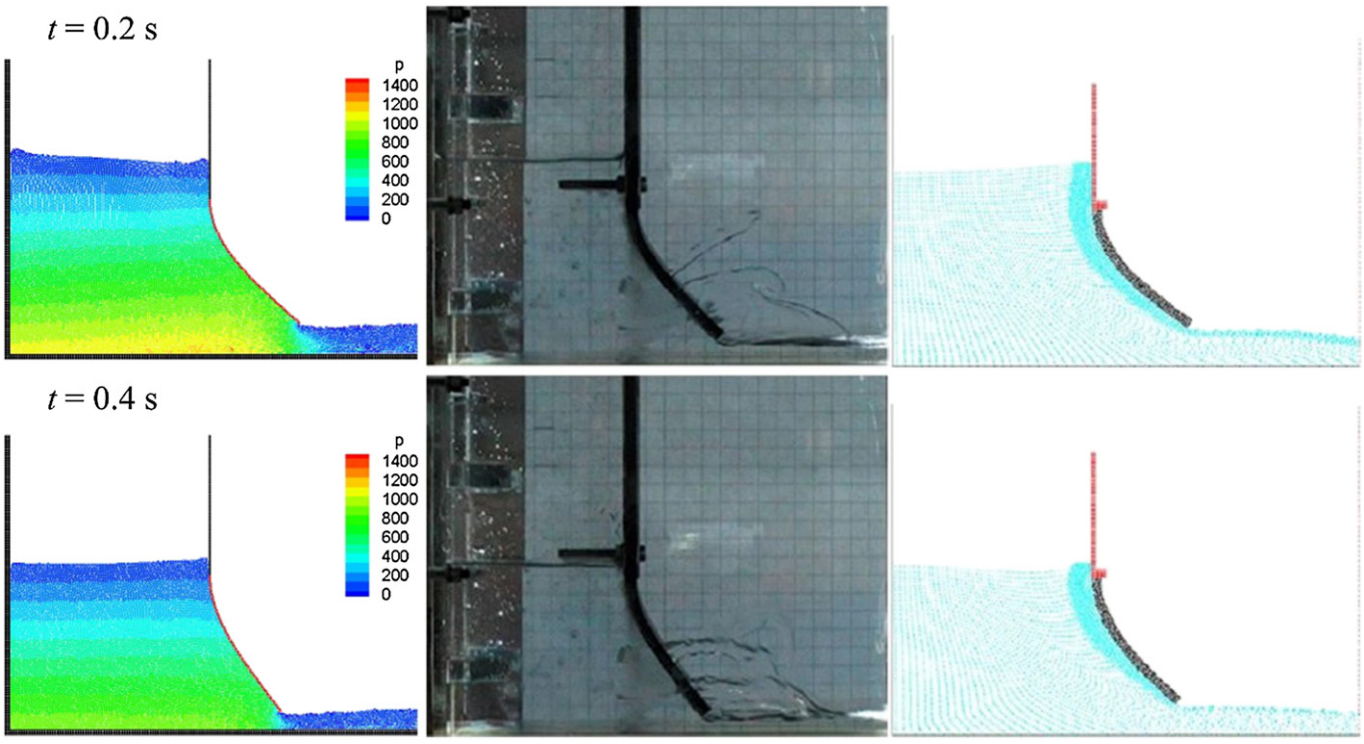

Fig. 5. Comparison of SPH–EBG (left) simulation with experiment (middle) and SPH (right) results from (Antoci et al., 2007) at time 0.2 s and 0.4 s. The color shows the pressure of the fluid.

over near neighbors because the kernel W vanishes outside its support domain. In this paper the cubic spline kernel function is used as follows

$$W(s,h)=\alpha_d\begin{cases}(2-s)^3-4(1-s)^3, & 0\le s<1\\ (2-s)^3, & 1\le s<2\\ 0, & s\ge 2\end{cases} \tag{5}$$

where $s=r/h$, r is the distance between two particles, α_d is a normalization factor, with the value of 1/6 h, $5/(14\pi h^2)$ and $1/(4\pi h^3)$ in one, two and three dimensional space, respectively.

The gradient of A can be obtained by differentiating Eq. (4) as

$$\nabla A_a=\sum_b \frac{m_b}{\rho_b}A_b\nabla_a W_{ab} \tag{6}$$

where $\nabla_a W_{ab}=W_{ab}'\mathbf{r}_{ab}/|\mathbf{r}_{ab}|$ is the gradient of the kernel taken with respect to the position of particle a, and $\mathbf{r}_{ab}=\mathbf{r}_a-\mathbf{r}_b$.

It is shown in Eqs. (4) and (6) that SPH provides a numerical approach for discretizing partial differential equations through operating on the smoothing function rather than on the field function itself. Applying SPH formulations (4) and (6), the Lagrangian form of the N–S Eqs. (1) and (2) can be written in the following SPH form

$$\frac{d\rho_a}{dt}=\sum_b m_b\mathbf{u}_{ab}\cdot\nabla_a W_{ab} \tag{7}$$

$$\frac{d\mathbf{u}_a}{dt}=\mathbf{g}_a-\sum_b m_b\left(\frac{P_a}{\rho_a^2}+\frac{P_b}{\rho_b^2}+\Pi_{ab}\right)\nabla_a W_{ab}+\sum_b\frac{m_b(\mu_a+\mu_b)\mathbf{r}_{ab}\cdot\nabla_a W_{ab}}{\rho_a\rho_b(r_{ab}^2+\eta)}\mathbf{u}_{ab} \tag{8}$$

where $\mathbf{u}_{ab}=\mathbf{u}_a-\mathbf{u}_b$, $\mathbf{r}_{ab}=\mathbf{r}_a-\mathbf{r}_b$, and $r_{ab}=|\mathbf{r}_{ab}|$. The term $\eta=0.01h^2$ is added to prevent singularities of the viscous term when two particles approach each other infinitely. Details of SPH formulations on the N–S equations can be found in many SPH references (Liu and Liu, 2003; Monaghan, 2005).

In order to reduce unphysical particle oscillations, an artificial viscosity Π_{ab} is employed (Monaghan, 1992)

$$\Pi_{ab}=\frac{-\alpha ch\mathbf{u}_{ab}\cdot\mathbf{r}_{ab}}{\overline{\rho}_{ab}(r_{ab}^2+\eta)},\qquad \mathbf{u}_{ab}\cdot\mathbf{r}_{ab}<0 \tag{9}$$

where $\overline{\rho}_{ab}=(\rho_a+\rho_b)/2$. The parameter α is the strength of the artificial viscosity. The artificial viscosity only works when neighboring particles approach each other, and it vanished when neighboring particles keep away from each other.

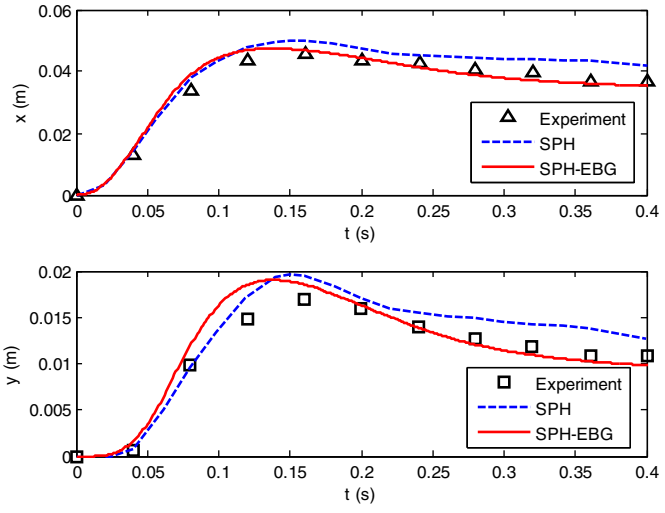

Fig. 6. Horizontal (x) and vertical (y) displacements of the free end of the gate, compared with the experimental and SPH results from Antoci et al. (2007).

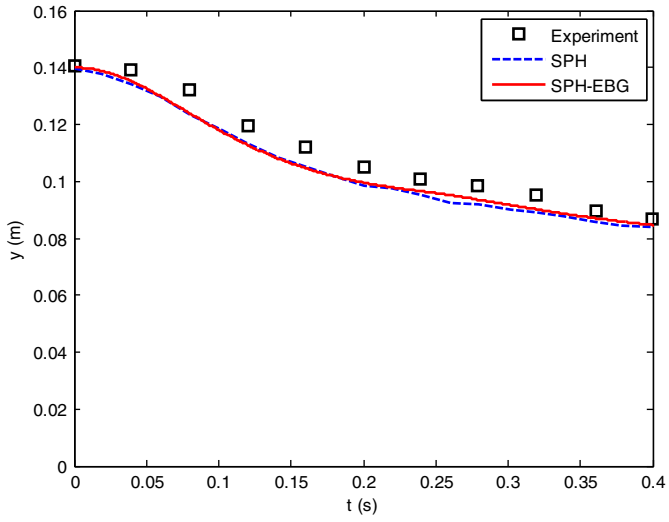

Fig. 7. Water level in the middle of the tank (5 cm far from the gate), compared with the experimental and SPH results from Antoci et al. (2007).

In order to model surface tension, an inter-particle force (Tartakovsky and Meakin, 2005; Yang et al., 2014) is added into the momentum Eq. (8) as follows

$$\frac{d\mathbf{u}_a}{dt} = \mathbf{g}_a - \sum_b m_b \left(\frac{P_a}{\rho_a^2} + \frac{P_b}{\rho_b^2} + \Pi_{ab}\right)\nabla_a W_{ab} + \sum_b \frac{m_b(\mu_a + \mu_b)\mathbf{r}_{ab}\cdot\nabla_a W_{ab}}{\rho_a \rho_b (r_{ab}^2 + \eta)}\mathbf{u}_{ab} + \sum_b \frac{\mathbf{F}_{ab}^I}{m_a} \tag{10}$$

where $\mathbf{F}_{ab}^I$ is the artificial inter-particle force acting on particle a due to particle b. The inter-particle force used in this paper is

$$\mathbf{F}_{ab}^I = \begin{cases} s_{ab}\dfrac{m_a + m_b}{2}\cos\left(\dfrac{1.5\pi}{kh}r_{ab}\right)\dfrac{\mathbf{r}_{ab}}{r_{ab}}, & r_{ab} \le kh \\ 0, & r_{ab} > kh \end{cases} \tag{11}$$

where s_{ab} is the strength of the force acting between particles a and b.

In SPH, an incompressible fluid can be treated as a slight compressible fluid using an artificial equation of state. In this paper, the following equation of state (Morris et al., 1997) is used

$$P(\rho) = c^2(\rho - \rho_0) \tag{12}$$

where ρ_0 is a reference density, c is a numerical speed of sound. In order to reduce the density fluctuation down to one percent c is usually taken ten times higher than the maximum fluid velocity (Morris et al., 1997).

In SPH simulations, there may be large fluctuation in the pressure field of particles because the density error accumulates when time marches. In order to reduce the fluctuation, some density correction approaches are proposed. In this paper, the Shephard filtering (Bonet and Lok, 1999) is used to reinitialize density every 25 time steps

$$\tilde{\rho}_a = \frac{\sum_b m_b W_{ab}}{\sum_b W_{ab} V_b}. \tag{13}$$

Since there are no particles that exist in the outer region of a free surface, the pressure of a particle on free surface should be equal to zero. If the pressure of the free surface particle does not equal zero, non-physical phenomenon may appear. In order to prevent the occurrence of non-physical phenomenon, the density will be set to reference density if a particle is on free surface, so its pressure will be zero according to the equation of state (12). A particle which satisfies

$$\sum_b W_{ab} V_b < \beta \tag{14}$$

is considered as a surface particle, where β is a parameter. In this paper $\beta = 0.9$. The free surface treatment used here is similar to that used in the moving particle semi-implicit (MPS) method (Koshizuka et al., 1998).

2.2. EBG method

In this paper, the movement and deformation of a flexible fiber are modeled by using the EBG method, which replaces the fiber with a layer of particles. Fiber particles can interact with neighboring fiber particles and fluid particles. In the EBG model, an EBG is made of two adjacent line segments connecting three neighboring particles, and the bending moment is converted to pairs of forces acting on the EBG particles (see Fig. 1) (Hosseini and Feng, 2009; Zhou and Wagoner, 1995).

According to Newton's second law of motion, the equation for a flexible fiber particle can be written as follows

$$m\frac{d\mathbf{u}}{dt} = \mathbf{T} + \mathbf{F}^B + \mathbf{F}^D + \mathbf{g} \tag{15}$$

where $\boldsymbol{T}$ denotes the tension acting on a fiber particle from adjacent points, $\boldsymbol{F}^B$ denotes the force due to EBG, and $\boldsymbol{F}^D$ denotes the fluid force from neighboring fluid (SPH) particles.

The tension can be calculated as

$$\mathbf{T}_{ba} = EA\left(\frac{r_{ab}}{r_{ab}^0} - 1\right)\frac{\mathbf{r}_{ab}}{r_{ab}} \tag{16}$$

where E and A are the Young's modulus and the cross-sectional area of the fiber, respectively, r_{ab}^0 is the reference distance between particles a and b. In order to reduce the length fluctuation down to one percent, EA is taken a magnitude of two orders higher than the maximum tension along the fiber.

The force $\mathbf{F}_{ba}^B$ acting on particle b from particle a due to EBG satisfies the follow equation

$$\mathbf{M}_b = \mathbf{r}_{ab} \times \mathbf{F}_{ba}^B \tag{17}$$

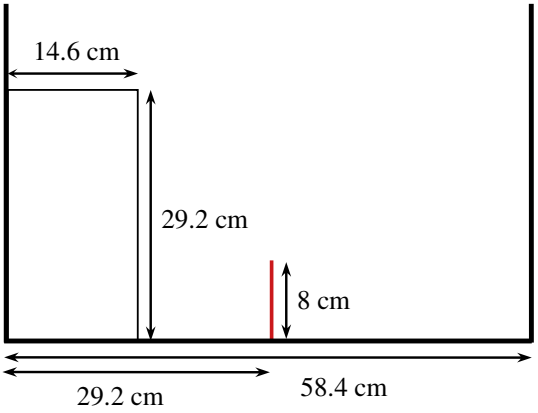

Fig. 8. Sketch of dam break with a bottom-fixed flexible plate.

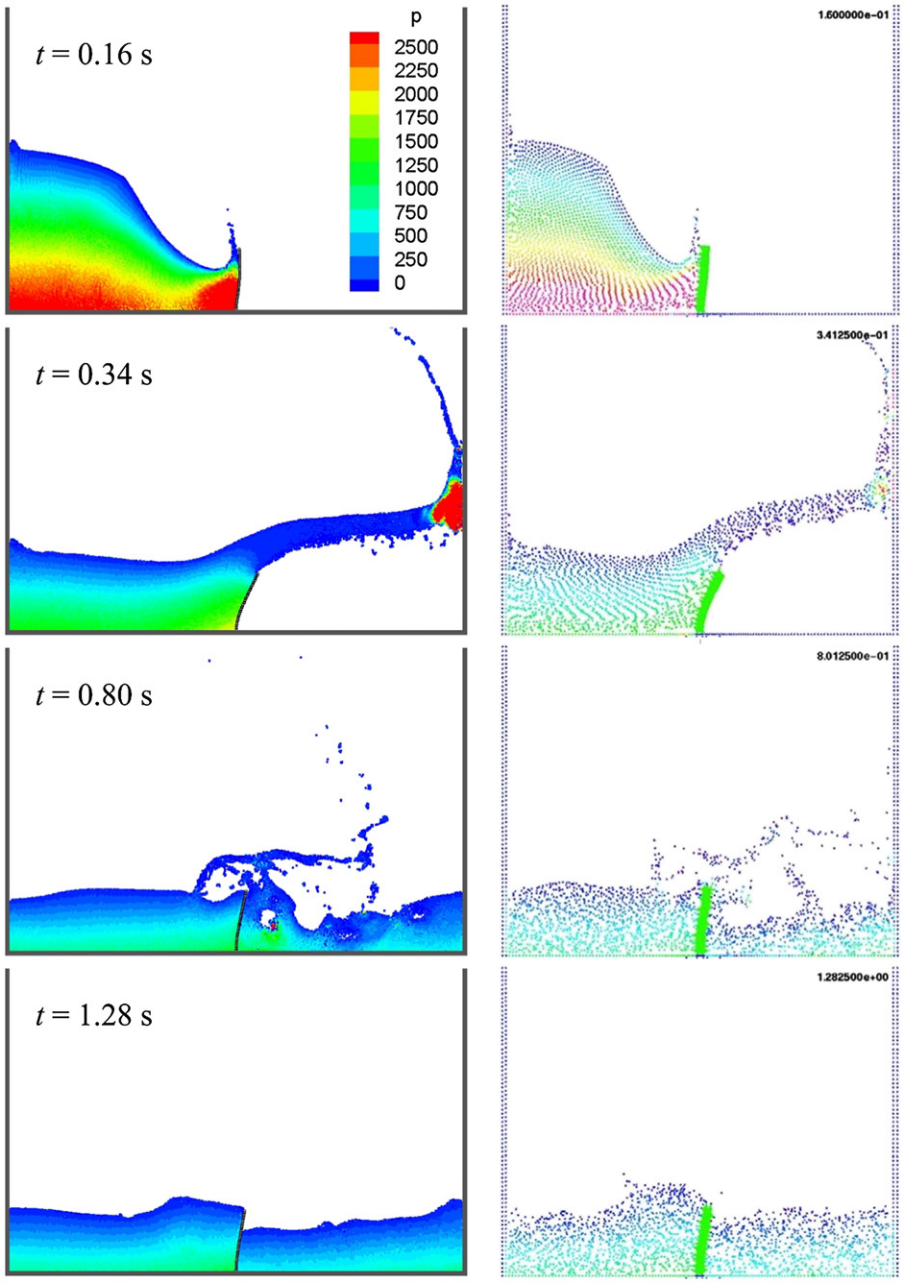

Fig. 9. Comparison of SPH–EBG (left) simulation with PFEM (right) results from (Idelsohn et al., 2008) at time 0.16 s, 0.34 s, 0.80 s, and 1.28 s. The color shows the pressure of the fluid.

where $\boldsymbol{M}_b$ denotes the moment acting on particle b (see Fig. 1), which is defined as

$$M_b = \frac{EI\left(\theta_b - \theta_b^0\right)}{r_{ba} + r_{bc}} \tag{18}$$

where EI and θ are the bending rigidity and the deflection of the flexible fiber, respectively. θ_b^0 is a reference deflection at particle b. The direction of $\boldsymbol{M}_b$ is determined by the value of $(\theta_b - \theta_b^0)$: it is clockwise if $(\theta_b - \theta_b^0)$ is negative and counter clockwise if $(\theta_b - \theta_b^0)$ is positive.

The total force acting on particle b due to EBG can be calculated as

$$\mathbf{F}_b^B = \mathbf{F}_{ba}^B + \mathbf{F}_{bc}^B - \mathbf{F}_{ab}^B - \mathbf{F}_{cb}^B \tag{19}$$

where $\mathbf{F}_{ba}^B$ and $\mathbf{F}_{bc}^B$ are from the EBG with particle b as a center, $-\mathbf{F}_{ab}^B$ is from the EBG with particle a as a center, and $-\mathbf{F}_{cb}^B$ is from the EBG with particle c as a center.

If particle b is at a free end and particle a does not exist, then the EBG with b as a center does not exist and the corresponding bending moment does not exist. So for a free end, the total force due to EBG is

$$\mathbf{F}_b^B = -\mathbf{F}_{cb}^B. \tag{20}$$

For a fixed end, movement and rotation are not allowed. Therefore, the bending moment at a fixed end should be defined. Assuming that there is a fixed line, ab, outside the fixed end b (see Fig. 2), and then the bending moment on particle b can be defined as

$$M_b = \frac{EI\left(\theta_b - \theta_b^0\right)}{r_{bc}}. \tag{21}$$

Then the total force acting a fixed end due to EBG is

$$\mathbf{F}_b^B = \mathbf{F}_{bc}^B - \mathbf{F}_{cb}^B. \quad (22)$$

2.3. Coupling of SPH and EBG

In SPH–EBG method, SPH particles are used to model the fluid flow and EBG particles are used to model the movement and deformation of the flexible structure. For modeling the fluid–flexible structure interaction, it is natural to couple SPH–EBG through allowing the interaction of neighboring fluid and structure particles (see Fig. 3). In other words, the particles of flexible structure are regarded as moving boundary in SPH. As fluid and structure particles are regarded as neighboring particles, it is natural to include structure particles in Eq. (10) when calculating forces acting on fluid particles. The force on a fiber particle from a neighboring fluid particle is then the same as the force on the fluid particle from the fiber particle except for the direction which is the opposite. As such, fiber particles can be regarded as a special type of SPH particles, on one hand, they can interact with regular SPH particles for fluids; on the other hand, they can interact with each other as EBG particles through taking account of the tension and bending force.

3. Numerical examples

The SPH–EBG coupling method will be validated in this section by applying it to model three different problems of dam-break on flexible structures.

3.1. Dam-break on a top-fixed flexible gate

In order to compare with experimental and numerical results, the computational settings of the example are similar to Antoci et al. (2007). The initial configuration of the example is shown in Fig. 4. A water column of width 0.1 m and height 0.14 is filled in a tank with a flexible gate of height 0.079 m on the right side. The gate is fixed at the upper end, while its lower end is free to move. The density of water is 1000 kg/m^3, and dynamic viscosity is 0.001 kg/s/m. The density of the gate is 1100 kg/m^3. Young's modulus of the gate is 1.2×10^7 N/m^2. The thickness of the gate is 5 mm. Then the corresponding bending rigidity of the gate is 0.125 N m. The system is at rest at initial time. According to gravity $g = 9.8$ m/s^2, the gate will experience a force from the water, then the flexible gate will bend and water will flow under it.

The system is simulated with initial particle spacing of 0.001 m, numerical sound speed of 50 m/s, and time step of 2×10^{-6} s. The computational domain is discretized with 13,635 fluid particles and 80 flexible gate particles. It should be noted that the flexible gate is modeled by a layer of EBG particles in our simulation, while it is a plate of thickness of 0.005 m in the experiment (Antoci et al., 2007). When the flexible gate bends, the length of the inner side (the left side) of the gate becomes slightly longer than the length of the outer side (the right side) of the gate. However, the corners of the free end are neglected in our simulation.

The SPH–EBG results are compared to experimental and SPH results (Antoci et al., 2007). As shown in Fig. 5, the flexible gate is deformed by the impulse of the fluid. The shapes of the free surface and the flexible gate are well simulated.

The displacements of the free end of the flexible gate are shown in Fig. 6, compared with the experimental and SPH modeling data from Antoci et al. (2007). It can be seen that the SPH–EBG results agree with the experimental results very well. It appears that the results of SPH–EBG are better than the SPH results except for the results before $t = 0.14$ s. It should be noted that the flexible gate experiences a friction along the lateral walls of the tank in the experiment (Antoci et al., 2007), while there is no such friction acting on the gate in a 2-dimensional simulations. Therefore, the gate moves faster in the simulation than in the 3D experiment. As shown in Fig. 6 the displacement of the free end in the simulation is larger than in the experiment when the gate moves out ward.

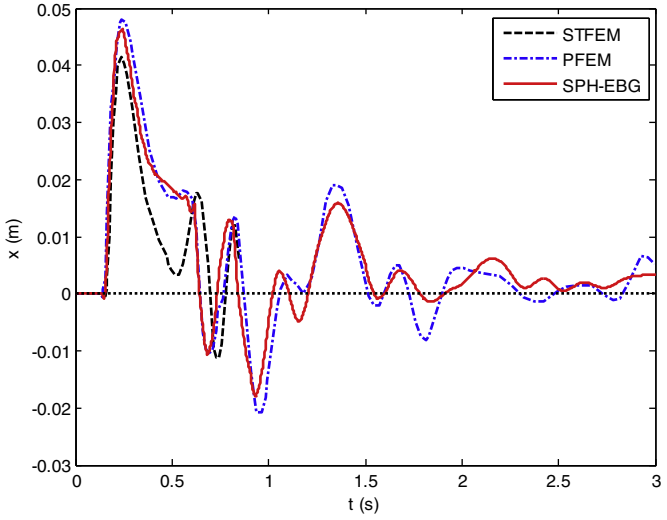

Fig. 10. Horizontal displacements of the free end of the flexible plate, compared with the results of STFEM (Walhorn et al., 2005) and PFEM (Idelsohn et al., 2008).

As to water level (see Fig. 7), the SPH–EBG results are very close to the SPH results, but slightly lower than the experimental results. The reason is that the vertical displacement of the free end in the simulation is larger than that in the experiment before the free end reaches its maximum displacement, and then there is more water flow under the free end of the gate.

3.2. Dam-break flow impacting on a bottom-fixed flexible plate

This case was simulated in order to validate that the SPH–EBG method presented in this paper can model violent free surface flow interacting with flexible structure. As shown in Fig. 8, a water column of width 14.6 cm and height 29.2 cm is placed in the left side of a tank. The width of the tank is 58.4 cm. A flexible plate of height 8 cm and width 1.2 cm is fixed at the middle of the tank. The upper end of the plate is free to move. The density of the plate is 2500 kg/m^3, and Young's modulus is 10^6 N/m^2.

The system is simulated with initial particle spacing of 0.002 m, numerical sound speed of 50 m/s, and time step of 4×10^{-6} s. The computational domain is discretized with 10,512 fluid particles and 41 flexible plate particles. This example is similar to Walhorn et al. (2005), and it was also simulated by Idelsohn et al. (2008). In this paper, the flexible

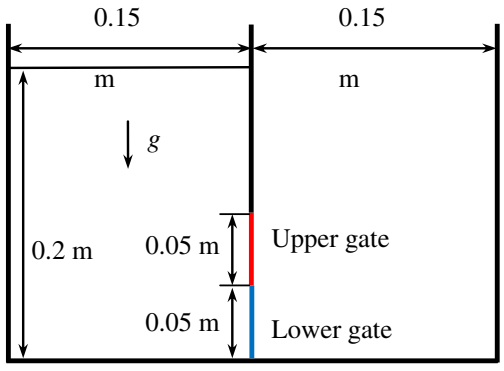

Fig. 11. Sketch of dam break with a top-fixed flexible gate (upper) and a bottom-fixed flexible gate (lower).

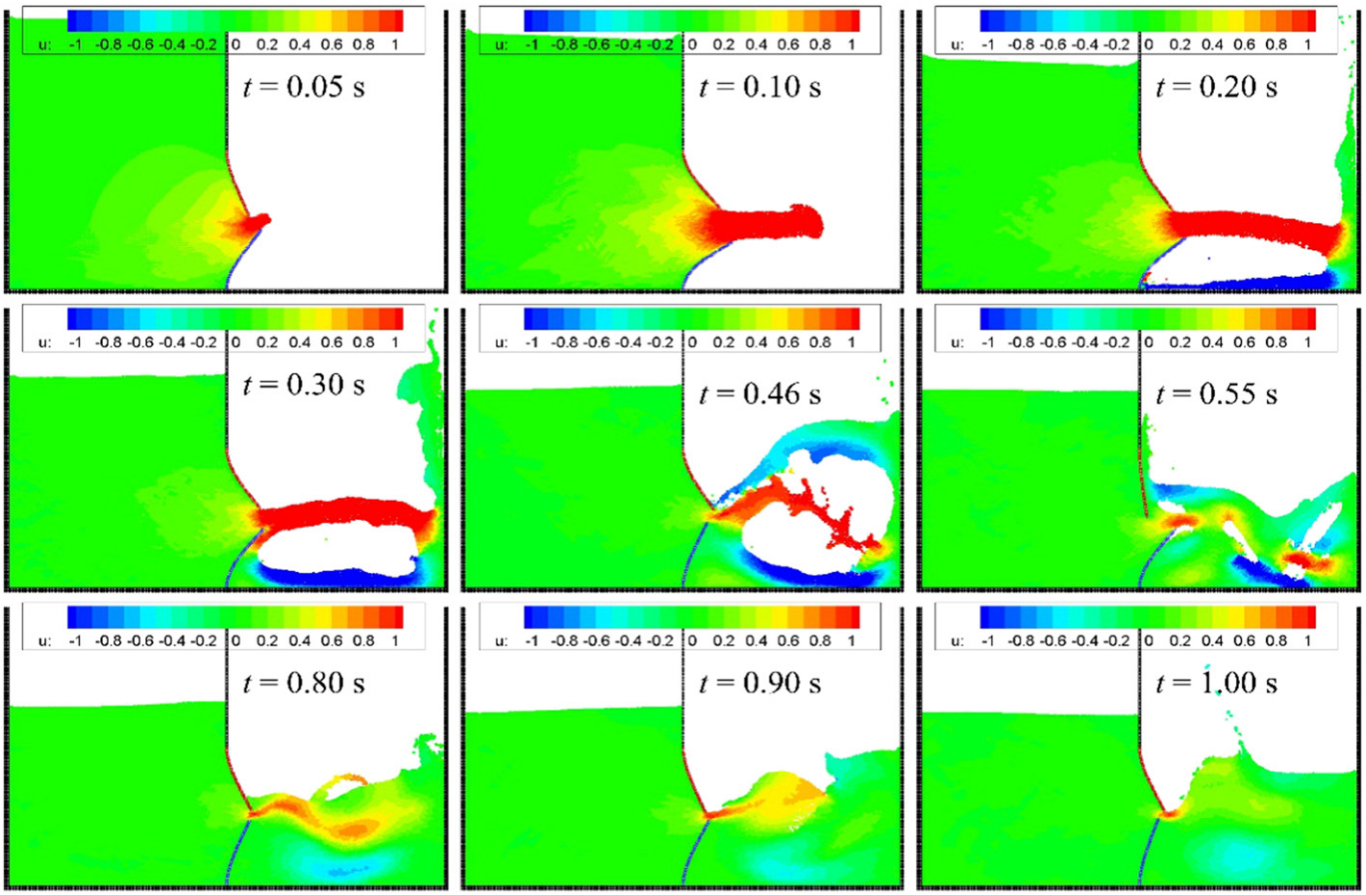

Fig. 12. The evolution of the dam break flow on a top fixed and a bottom fixed flexible gates. The color shows the horizontal velocity of the flow field.

plate is replaced by a layer of EBG particles. Simulations with different values of bending rigidity were run. The results of the simulation with EI = 0.29 N m, which agrees with Idelsohn et al. (2008), are discussed in the following.

The SPH–EBG results are compared to PFEM results (Idelsohn et al., 2008) in Fig. 9. In general, the results of SPH–EBG and PFEM agree with each other. However, the particle distribution of SPH–EBG results is more uniform than that of the PFEM results, especially in the area near the free surface and wall boundary. It is also shown in Fig. 9 that the dam break flow impacting on a flexible plate is very complex. Before the flow reaches the plate, it is the same as an ordinary dam break flow. When the flow impacts on the plate, the free end of the plate first moves to left, and then moves to the right while the fluid rises and passes the top end of the plate. After impacting on the right wall of the tank, the flow goes back along the bottom and then impacts on the right side of the flexible plate. Then the fluid from both sides of the plate interacts with each other and the flow becomes very violent and complex.

The horizontal displacements of the free end of the flexible plate are shown in Fig. 10, compared with the results obtained by space–time finite element method (STFEM) (Walhorn et al., 2005) and particle finite element method (PFEM) (Idelsohn et al., 2008). It should be noted that the STFEM and PFEM results are the displacements of the left corner of the free end of the plate. In general, the SPH–EBG results agree with PFEM results before about $t = 1.7$ s but not well agree with STFEM results. It can be seen that the free end of the plate reaches a maximum displacement to the right at about $t = 0.25$ s, and then it returns back. Then the plate experiences a rapid oscillation, and the free surface is very complex (see Fig. 9). At about $t = 0.95$ s the free end of the flexible plate reaches a maximum displacement to the left. After about $t = 1.5$ s the system calms down gradually.

3.3. Dam-break on a top-fixed and a bottom-fixed flexible gates

The initial configuration of the example is shown in Fig. 11. A water column of width 0.15 m and height 0.2 m is filled in a tank with a top-fixed flexible gate of height 0.05 m and a bottom-fixed flexible gate of height 0.05 m on the right side. The length of the tank is 0.3 m. The top-fixed gate is fixed at the upper end, while its lower end is free to

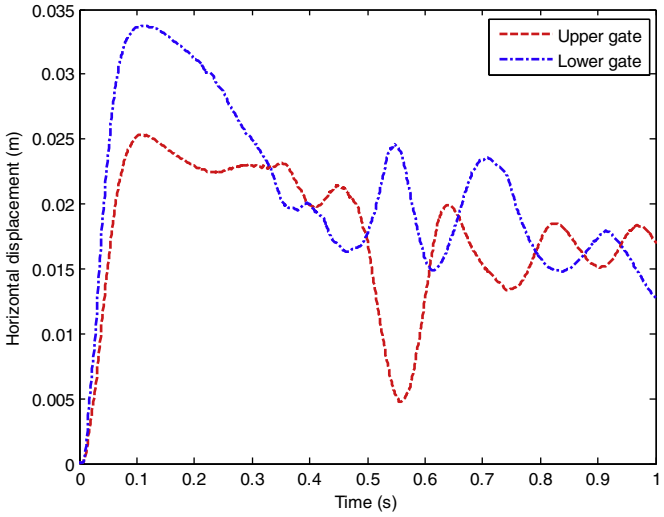

Fig. 13. Horizontal displacements of the free ends of the upper and lower gates.

move. The bottom-fixed gate is fixed at the lower end, while its upper end is free to move. The density of water is 1000 kg/m^3, and dynamic viscosity is 0.001 kg/ms. The density of the gate is 1100 kg/m^3. Young's modulus of the gate is 1.0×10^7 N/m^2. The bending rigidity of the gate is 0.05 N m. The system is at rest at initial time.

The system is simulated with initial particle spacing of 0.001 m, numerical sound speed of 50 m/s, and time step of 2×10^{-6} s. The computational domain is discretized with about 30,000 fluid particles and 100 flexible gate particles.

The evolution of the dam break on two gates is shown in Fig. 12. As the flexible gates experience a force from the water, the gates bend to open and the water jets out of the gates (Fig. 12, $t = 0.05$ s and 0.1 s). After impacting on the right wall of the tank and going back (Fig. 12, $t = 0.2$ s), the water flows along the right side of the bottom plate and merges with the jet (Fig. 12, $t = 0.3$ s). After a violent interaction of the flow and the gates (Fig. 12, $t = 0.46$ s and 0.55 s), the water on the right side forms a pool whose depth is higher than the jet (Fig. 12, $t = 0.8$ s). Then the water level of the right side increases, while the water level of the left side still decreases until a balance is reached.

The horizontal and vertical displacements of the free ends of the upper and the lower gates are shown in Figs. 13 and 14, respectively. For both the upper and the lower gates, the positive horizontal displacements mean the free ends move to right, while the positive vertical displacements mean the free ends move up. Since the free end of the lower gate moves down in vertical direction as shown in Fig. 12, its vertical displacement is negative as shown in Fig. 14. At the first stage of dam break, both the upper and lower gates bend toward the right side quickly. As the fluid pressure on the lower gate is larger than that on the upper gate, the lower gate moves faster than the upper gate. At about time $t = 0.1$ s, both the upper and the lower gates reach their maximal horizontal displacements. Then the lower gate moves back, while the upper gate only moves back a little. At about time $t = 0.33$ s, the displacements of the two gates are very close to each other. Then the gates experience oscillations of nearly the same frequency. In general, if the oscillation is not considered, the displacements decrease with time after $t = 0.1$ s, because the water level of the left side decreases while the water level of the right side increases with time.

Fig. 15 shows the distances between the free ends of the upper and lower gates. The vertical and horizontal distances are defined as

$$x = x_l - x_u,\ y = y_u - y_l \tag{23}$$

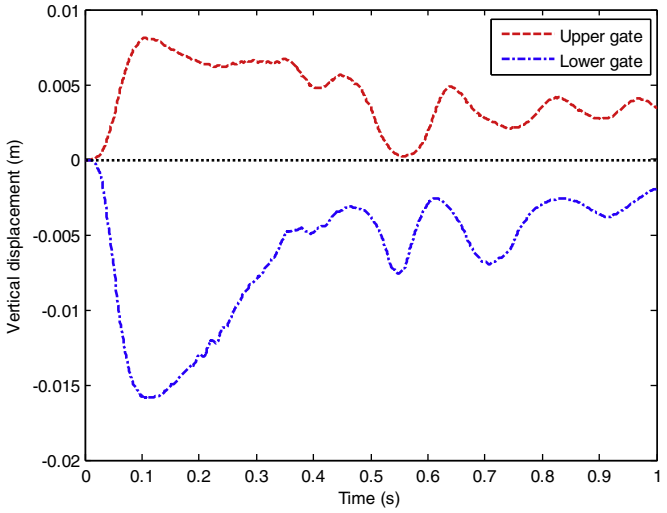

Fig. 14. Vertical displacements of the free ends of the upper and lower gates.

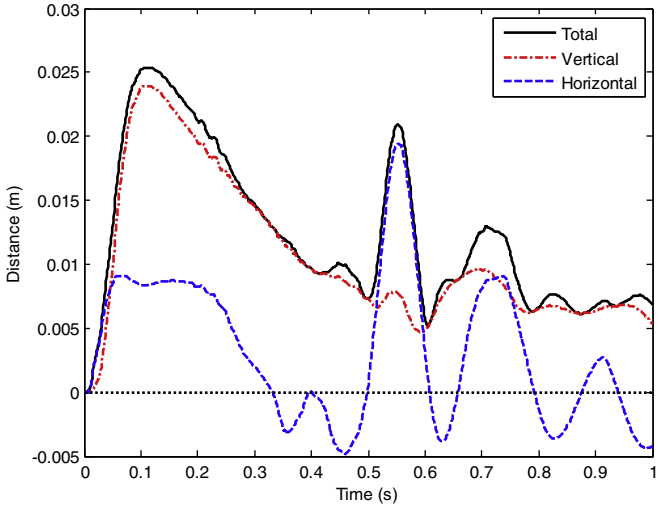

Fig. 15. The distances between the free ends of the upper and lower gates. The 'total' is the distance between the free ends. The 'vertical' and 'horizontal' are components of the distance in vertical and horizontal directions, respectively.

where the subscripts l and u denote the lower and the upper gates, respectively. Then the total distance is $d = \sqrt{x^2 + y^2}$. The minus value of horizontal distance shown in Fig. 15 means the horizontal displacement of the upper gate is larger than that of the lower gate. It is shown that the distance is mainly in vertical direction for most of the time while the oscillation of the distance is mainly in horizontal direction.

4. Conclusions and discussions

In this paper, an improved SPH–EBG coupling method is developed for modeling the interaction of fluid with free surface and flexible structure with free and fixed ends. SPH is used to represent the fluid, EBG is used to represent the flexible structure, and the fluid–flexible structure interaction is implemented through allowing the interaction of neighboring SPH and EBG particles. As both SPH and EBG are Lagrangian particle methods, the coupling of SPH and EBG is naturally Lagrangian. A fixed-end treatment is introduced for flexible structures. A free surface treatment and a surface tension model are used for free surface flow.

The SPH–EBG method possesses two advantages. Firstly the SPH–EBG method combines the best features of SPH and EBD, and therefore it is capable of modeling interactions of viscous fluid with or without free surface and flexible structure with large deformation, as shown in the numerical examples. Secondly, in SPH–EBG model, a flexible structure is replaced by a layer of EBG particles, and it can simulate a flexible structure of very small thickness. For a structure, if the length is much large compared with its thickness, the thickness of the structure may be neglected, as far as fluid–structure interaction is concerned. This is advantageous comparing to other approaches. For example, if SPH particles are also used to model the movement and deformation of flexible structures, a quite large number of particles need to be deployed on the structure. As EBG uses only a layer of particles, the computational cost can be greatly reduced.

The improved SPH–EBG method is applied to simulate problems of dam break flow on flexible structures. The flexible structures in all numerical cases of the present work have fixed ends and free end. As the dam break flow impacts on the flexible structure, the structure experiences large deformations. As a result, the free end of the structure moves back and forth. The SPH–EBG results are compared with experimental or/and numerical results from other sources. The good agreement of the results show that the numerical method presented in this paper is accurate and reliable.

Acknowledgment

This work was supported by the National Natural Science Foundation of China (Grant No. 11302237 and No. 11172306) and NSAF (Grant No. U1530110).

Appendix A. Supplementary data

Supplementary data to this article can be found online at http://dx.doi.org/10.1016/j.coastaleng.2015.11.007.

References

Antoci, C., Gallati, M., Sibilla, S., 2007. Numerical simulation of fluid–structure interaction by sph. Comput. Struct. 85 (11), 879–890.
Baaijens, F.P., 2001. A fictitious domain/mortar element method for fluid–structure interaction. Int. J. Numer. Methods Fluids 35 (7), 743–761.
Bonet, J., Lok, T.-S., 1999. Variational and momentum preservation aspects of smooth particle hydrodynamic formulations. Comput. Methods Appl. Mech. Eng. 180 (1), 97–115.
Breinlinger, T., Polfer, P., Hashibon, A., Kraft, T., 2013. Surface tension and wetting effects with smoothed particle hydrodynamics. J. Comput. Phys. 243, 14–27.
Gingold, R.A., Monaghan, J.J., 1977. Smoothed particle hydrodynamics: theory and application to non-spherical stars. Mon. Not. R. Astron. Soc. 181, 375–389.
Hosseini, S.M., Feng, J.J., 2009. A particle-based model for the transport of erythrocytes in capillaries. Chem. Eng. Sci. 64 (22), 4488–4497.
Hu, X.Y., Adams, N.A., 2007. An incompressible multi-phase sph method. J. Comput. Phys. 227 (1), 264–278.
Idelsohn, S.R., Marti, J., Limache, A., Oñate, E., 2008. Unified lagrangian formulation for elastic solids and incompressible fluids: application to fluid–structure interaction problems via the pfem. Comput. Methods Appl. Mech. Eng. 197 (19), 1762–1776.
Koshizuka, S., Nobe, A., Oka, Y., 1998. Numerical analysis of breaking waves using the moving particle semi-implicit method. Int. J. Numer. Methods Fluids 26 (7), 751–769.
Liu, G.R., Liu, M.B., 2003. Smoothed Particle Hydrodynamics: A Meshfree Particle Method. World Scientific, Singapore.
Lucy, L.B., 1977. A numerical approach to the testing of the fission hypothesis. Astron. J. 82, 1013–1024.
Marrone, S., Colagrossi, A., Antuono, M., Colicchio, G., Graziani, G., 2013. An accurate sph modeling of viscous flows around bodies at low and moderate reynolds numbers. J. Comput. Phys. 245, 456–475.
Monaghan, J.J., 1992. Smoothed particle hydrodynamics. Annu. Rev. Astron. Astrophys. 30, 543–574.
Monaghan, J.J., 2005. Smoothed particle hydrodynamics. Rep. Prog. Phys. 68, 1703–1759.
Morris, J.P., Fox, P.J., Zhu, Y., 1997. Modeling low Reynolds number incompressible flows using sph. J. Comput. Phys. 136 (1), 214–226.
Tartakovsky, A., Meakin, P., 2005. Modeling of surface tension and contact angles with smoothed particle hydrodynamics. Phys. Rev. E 72 (2), 026301.
Tsubota, K.-i., Wada, S., Yamaguchi, T., 2006. Simulation study on effects of hematocrit on blood flow properties using particle method. J. Biomed. Sci. Eng. 1 (1), 159–170.
Walhorn, E., Kölke, A., Hübner, B., Dinkler, D., 2005. Fluid–structure coupling within a monolithic model involving free surface flows. Comput. Struct. 83 (25), 2100–2111.
Yang, X., Liu, M., Peng, S., 2014. Smoothed particle hydrodynamics and element bending group modeling of flexible fibers interacting with viscous fluids. Phys. Rev. E 90 (6), 063011.
Yu, Z., 2005. A dlm/fd method for fluid/flexible-body interactions. J. Comput. Phys. 207 (1), 1–27.
Zhou, D., Wagoner, R., 1995. Development and application of sheet-forming simulation. J. Mater. Process. Technol. 50 (1), 1–16.
Zhu, L., Peskin, C.S., 2003. Interaction of two flapping filaments in a flowing soap film. Phys. Fluids 15 (7), 1954–1960.

View publication stats